Construction of a Stable Dimer of *Bacillus stearothermophilus* Lactate Dehydrogenase†

Richard M. Jackson,*,‡ Josep L. Gelpi,§ Antonio Cortes,§ David C. Emery,‡ Helen M. Wilks,‡ Kathleen M. Moreton,‡ David J. Halsall,‡ Roger N. Sleigh,‡ Moira Behan-Martin,∥ Gareth R. Jones,∥ Anthony R. Clarke,‡ and J. John Holbrook‡

Molecular Recognition Centre and Department of Biochemistry, University of Bristol School of Medical Sciences, Bristol BS8 1TD, U.K., Department of Biochemistry and Physiology, University of Barcelona, Martí y Franquès 1, 08028 Barcelona, Spain, and SERC Daresbury Laboratory, Daresbury, Warrington WA4 4AD, U.K.

Received December 2, 1991; Revised Manuscript Received May 28, 1992

ABSTRACT: A molecular graphics analysis of the features which prevent cytosolic malate dehydrogenase dimers from forming tetramers was evaluated by its success in predicting the synthesis of a version of the LDH framework which is a stable dimer. Surface residues responsible for malate dehydrogenases being dimers were revealed by superimposing the structures of two dimers of pig cytosolic malate dehydrogenase on one homologous tetramer of L-lactate dehydrogenase from *Bacillus stearothermophilus*. Four regions were identified as composing the *P*-axis dimer–dimer interface. Two regions of the dimer were surface loops that collided when built as a tetramer: a large loop (residues 203–207, KNOBI) and a small loop (residues 264–269, KNOBII), and these were candidates to explain the dimeric character of malate dehydrogenase. The analysis was tested by constructing a synthetic *B. stearothermophilus* lactate dehydrogenase (KNOBI) containing the large malate dehydrogenase loop (residues 203–207 being AYIKLQAKE, and extra four amino acids). The new construct was thermotolerant (90 °C) and enzymically active with k_{cat} and K_M (pyruvate) values similar to those of the wild-type enzyme. However, whereas the allosteric activator fructose 1,6-bisphosphate decreased K_M 100 times for wild type, it had no influence on KNOBI. The molecular volumes of 1–120 μM concentrations of the construct were measured by time-resolved decay of tryptophan fluorescence anisotropy and by gel filtration. Both methods showed the molecular weight of wild type increased from dimer to tetramer with K_d about 20 μM dimer. KNOBI remained a dimer under these conditions. In the presence of 1 mM fructose 1,6-bisphosphate wild type was stabilized as tetramer with K_d decreased to about 100 nM. KNOBI did not form a tetramer with $K_d < 130$ μM dimer either with or without the effector. It is concluded that presence of a large surface loop is a determinant for cytosolic malate dehydrogenase being a dimer.

Many enzymes, such as the NAD^+-dependent L-hydroxy acid dehydrogenases, exist as oligomers of identical subunits or of closely related isoforms (Rossmann et al., 1975). By synthesis of simple (monomeric) protein catalysts we seek to understand the advantages or otherwise of the oligomeric state. Advantage is usually ascribed either to increased protein stability from a greater buried hydrophobic core or to the potential for regulation by site–site interaction across subunit interfaces. The LDH/cMDH[1] family of enzyme offers a good system with which to experimentally test the putative advantages of the oligomeric state: both classes of enzyme have superimposable tertiary (subunit) structures and essentially the same mechanism of enzyme action, but the LDHs are typically stable tetramers (Holbrook et al., 1975), whereas the cMDHs are usually dimers (Banaszak & Bradshaw, 1975). At very high protein concentrations all subunits associate, and at infinitely low protein concentration all oligomers will dissociate. In this paper the word "stable" relates to assembly state relative to physiological protein concentration (ca. 30 μM).

A search for species-independent structural features which determine the oligomeric state could identify (a) positive interactions which stabilize the LDH tetramer and (b) negative interactions which prevent the cMDH dimers from further associating to tetramers. Since our goal is to make simple catalysts, we do not emphasize the features which stabilize the mammalian LDH tetramers but state these are thought to be largely due to the four long N-terminal arms which extend between the pairs of dimers in LDH and which are much shorter in the dimeric cMDHs (Rossmann et al., 1975). When the first six residues of the N-terminal arm are removed proteolytically (Jeckel et al., 1973; Opitz et al., 1981; Pfleiderer et al., 1991), the pig tetramer becomes a thermally labile dimer. While that explanation is adequate for tetrameric mammalian LDHs, it cannot apply to the majority of the bacterial LDHs (most of which have only been characterized since these generalizations were made) since these are typically stable tetramers but like the MDHs lack the first 14–20 N-terminal residues which make up the *R*-axis "arm" in mammalian LDHs.

In this paper we present results of a molecular graphics analysis of the features which prevent MDH dimers from forming tetramers and then check the analysis by its success in predicting the synthesis of a version of the LDH framework which is a stable dimer. The enzymic and regulatory properties

† The work was supported by the Science and Engineering Research Council (U.K.), SmithKline Beecham Research (U.K.) Ltd., The British Council, and the Spanish Ministry of Science.

* Author to whom correspondence should be addressed.
‡ Molecular Recognition Centre, Bristol.
§ Department of Biochemistry, Barcelona.
∥ SERC Daresbury Laboratory.

[1] Abbreviations: LDH, L-lactate dehydrogenase; MDH, L-malate dehydrogenase; cMDH, cytosolic isoenzyme of MDH; TEA, triethanolamine hydrochloride; FBP, fructose 1,6-bisphosphate.

0006-2960/92/0431-8307$03.00/0

of the synthetic dimer are compared to those of the wild-type tetramer. The thermostable LDH from *Bacillus stearothermophilus* was used for the construction since it can be easily reconstructed (Barstow et al., 1986) and, unlike most bacterial LDHs which are stable tetramers, its allosteric activation by FBP is in part linked to the change from unstable dimer to tetramer with a dissociation constant close to the physiological concentration of the enzyme [see Clarke et al. (1989) for a brief review]. Thus, the dimer–dimer surfaces are already evolved to be relatively stable in water, and we are not faced with the otherwise expensive and laborious task of making a gene to code for a new surface which must have about the same tertiary structure in water as it originally had when in contact with another hydrophobic surface. The complexity of that task is evident in the preliminary experiments of Steffan and McAlister-Henn (1991) aimed at obtaining monomers of the normally dimeric yeast mitochondrial MDH.

MATERIALS AND METHODS

Computational and Sequence Alignment Methods. The atomic coordinates of dimeric pig cytosolic MDH binary complex with NAD^+ were taken from release 53 of the Brookhaven Protein Database (Bernstein et al., 1977) with the correct amino acid sequence (Birktoft et al., 1989), those of the tetrameric *B. stearothermophilus* LDH ternary complex with NADH, oxamate, and FBP were from Wigley et al. (1992), and those of tetrameric pig M_4 LDH ternary complex with NADH and oxamate were from Dunn et al. (1991). The programs INSIGHT and DISCOVER were used to view structures and perform molecular mechanics calculations, respectively (Biosym Technologies, San Diego, CA) on a Silicon Graphics personal IRIS 4D-20 workstation and on an IBM 3090 computer with 150S vector processor. Energy calculations were carried out using the all atom consistent valence force field (Dauber-Osguthorpe et al., 1988). Amino acid sequence alignment was done manually with reference to regions of conserved secondary structure. This defined the structurally conserved regions and also variable-length loop regions of the LDH/MDH framework. The residues used in the alignment of cMDH and of both *B. stearothermophilus* and pig M_4 LDH are listed in Figure 1 and were used to model a cMDH tetramer by superposition of two cMDH dimers onto the pig and *B. stearothermophilus* LDH tetramers. The amino acid contacts across the *Q*-, *P*-, and *R*-axis subunit interfaces were calculated for given cutoff distances for both the authentic LDH and the model MDH tetramers. This identified collisions in the model across a given subunit interface.

A template forcing minimization routine (Struthers et al., 1984) was used to force the backbone atoms in flanking regions at either side of the cMDH loops to adopt the backbone conformation (template) in (i) the crystal structure *B. stearothermophilus* LDH and (ii) the crystal of cMDH, as a control. Residues in the loop regions (KNOBI and KNOBII) were allowed full conformational flexibility. Only valence and van der Waals energies were considered. The template-forced cMDH loop conformations which were now compatible with the backbone structure of the *B. stearothermophilus* LDH crystal were now modeled into this structure. Those residues from the original bsLDH structure that showed on graphics inspection a conformation incompatible with the inserted loop were changed to those in the corresponding cMDH sequence. This model structure was relaxed by steepest descents followed by conjugate gradients minimization until an rms derivative of <1 kcal mol^{-1} $Å^{-1}$ was reached. A 10-Å layer of water was placed around the loops and minimization continued to an average rms derivative of <0.002 kcal mol^{-1} $Å^{-1}$. All residues within 10 Å of the inserted loop were unconstrained; the remaining residues were fixed at their crystallographic positions. In this minimization a dielectric constant of 1 and charged group parametrization were used.

Table I: Sequence of the Mutagenic Oligonucleotides, Together with the Wild-Type *B. stearothermophilus* LDH Sequence and the Extended Loop Sequences Used To Construct the KNOBI Version of the Bacterial Gene and Protein

```
5'AGCCAGGCTTATATCAAACTCCAAGCTAAAGAGATGCCGATCCGCAAG3'

3'TCGGTCCGAATATAGTTTGAGGTTCGATTTCTCTACGGCTAGGCGTTC5' (mutagen)

  SerGlnAlaTyrIleLysLeuGlnAlaLysGluMetProIleArgLys   (KNOBI)

  SerGlnAlaTyrIleGly----------ValMetProIleArgLys     (wild type)
```

Genetic Manipulation Procedures. In general these used methods described by Sambrook et al. (1989). Restriction endonucleases, DNA ligases, and other DNA-modifying enzymes were obtained from Boehringer Corp. Ltd. and used in the buffers and under the conditions recommended by the supplier. Oligonucleotide site-directed mutagenesis was performed essentially as described by Carter et al. (1985). Oligodeoxynucleotides for site-directed mutagenesis and DNA sequencing were synthesized using a Du Pont Coder 300 DNA synthesizer. The oligonucleotide used for mutagenesis and the wild-type and new loop sequences are shown in Table I. The template used was a bacteriophage M13mp8 (Messing & Vieira, 1982) with the *B. stearothermophilus* LDH gene (Barstow et al., 1986) inserted between the *Eco*RI and *Pst*I sites which was purified from *Escherichia coli* TG2 (*lac-pro*, *sup*E, *thi*, *hsd*D5, [F'*tra*D36, *pro*AB, *lac*I^Q, *lac*Z M15]). *E. coli* BMH71-18*mut*L (*lac-pro*, *sup*E, *thi*, *hsd*D5, [F'*pro*AB, *lac*I^Q, *lac*Z M15], *mut*L::Tn10) was used as a host for transformation of M13mp8 containing the LDH gene after chain extension and ligation. *E. coli* TG2 was used as a host for transformation and expression of LDH genes in plasmid pKK223-3 (Brosius & Holy, 1984; Pharmacia P-L, Uppsala, Sweden) as described for pLDH41 (Barstow et al., 1986). Base sequence determinations were made by the chain termination procedure of Sanger et al. (1980). The synthetic gene was resequenced using a Du Pont Genesis 2000 automated sequencer and revealed only the desired mutations (data not shown).

Purification of the KNOBI Mutant of LDH from E. coli. Transfected cells were grown in 2xYT broth containing ampicillin (to select for the plasmid), were harvested by centrifugation, and were resuspended in 50 mM TEA/NaOH buffer (pH 6) and lysed by sonication. The mutant enzyme was precipitated by adding 0.43 g of $(NH_4)_2SO_4$/mL supernatant and recovered by centrifugation. The pellet was dissolved in a minimum volume of 50 mM TEA buffer (pH 6) and dialyzed against 50 volumes of that buffer overnight at 4 °C. The dehydrogenase was purified by affinity chromatography on an 8 cm^2 × 6 cm column of oxamate–agarose in 0.4 mM NADH. The enzyme was eluted with 50 mM TEA adjusted to pH 9.3 containing 0.5 M NaCl (without NADH) and was finally purified by ion-exchange chromatography on Q-Sepharose Fast Flow column and eluted with a 0–0.4M NaCl gradient and stored as the precipitate formed when 0.43 g of $(NH_4)_2SO_4$/mL of eluate was added. The sample gave a single band of apparent M_r 33 000 on sodium dodecyl sulfate PHAST (Pharmacia) gel electrophoresis calibrated with pig LDH and was judged from the Coomassie Blue staining to be >98% homogeneous. The yield was 150 mg of LDH/L of *E. coli* culture broth.

Steady-State Kinetics. Steady-state measurements were made by following the change in absorbance at 340 nm in the NADH/NAD^+ conversion. All assays were at 25 °C and in 20 mM BisTris–50 mM KCl buffer (pH 6) (note this is a different and better pH 6 buffer than used in much of our earlier work. Determination of k_{cat} and K_M for pyruvate was made at saturating NADH concentrations (0.2 mM). The results were fitted to a simple hyperbola or to a quadratic (when the constant for inhibition by pyruvate was also being measured) in pyruvate by nonlinear regression analysis using the Marquart–Levenburg algorithm (Marquart, 1963) implemented in GraFit v. 2 (Leatherbarrow, 1990). The enzyme concentration used was 6 nM subunits. Temperature stability measurements were carried out by incubating 5 μM LDH subunits at 90 °C in the above buffer. At intervals aliquots were removed, rapidly cooled, and assayed in the conditions described above.

Equilibrium Fluorescence Measurements. An SLM 8000 single photon counting spectrofluorometer was used to record the percent increase in counts with excitation at 297 nm and emission at 345 nm (4-nm slits) when 5 mM FBP was added to 2–180 μM subunits solution of wild-type enzyme in 20 mM BisTris-HCl–50 mM KCl (pH 6.0) at 25 °C.

Time-Resolved Fluorescence Anisotropy. Measurements utilized the time-correlated single photon counting fluorometer constructed on Port HA12 of the SERC Synchrotron Radiation Source at Daresbury with the ring running in the single bunch mode, as we previously described (Clarke et al., 1985). The time-to-analogue converter was used in the reverse mode: that is, it was triggered by a fluorescence photon and was stopped by the next pulse from a strip line on the ring. The polarized excitation was at 297 nm through a Spex monochromator and an angled interference filter. The emission was through a Melles Griot WG 335-nm cuton filter and an analyzing prism with motorized rotation from horizontal to vertical each 60 s. The time of acquisition was altered with protein concentration to give about 50 000 counts in the peak channel. The lamp pulse was obtained from a Ludox suspension. The *g* factor for the arrangement was 1.004. The synchrotron source gave far higher counting rates and final accuracy than were obtainable with a laboratory flash lamp source.

Gel Filtration. The apparent molecular weight of the LDHs was estimated using a Bio-Rad Bio-Sil TSK-250 HPLC gel filtration column equilibrated with 0.125 M NaCl and 50 mM TEA (pH 6) at 25 °C. The steel jacketed column was operated with mechanical injection within a fully automated Pharmacia FPLC apparatus which allowed the elution volumes to be repeated to ±0.05 mL. The applied protein was approximately 2.5, 10, 80, and 120 μM (as monomers). The column was calibrated under the same conditions using Bio-Rad gel filtration molecular weight standard 151-1901 containing thyroglobulin, IgG, ovalbumin, myoglobin, and cyanocobalamin.

RESULTS AND DISCUSSION

Structure, Sequence Analysis, and Modeling. The first step was to align the LDH and MDH sequences by overlapping those homologous regions of conserved secondary structure which are underlined in Figure 1. The rms deviations from superimposing Cα atms of the cMDH monomer on each of pig M_4 and *B. stearothermophilus* LDH monomers were 1.4 and 1.5 Å, respectively, and for the dimer were 1.9 and 2.2 Å, respectively. The rms deviations from superimposing pig M_4 on *B. stearothermophilus* LDH were 0.85 and 0.90 Å for the monomer and dimer, respectively. Hence, conserved secondary structure elements and variable-length surface loops were well-defined [as was expected from early work (Rossmann et al., 1975) with less accurate structures]. It became immediately evident from superimposition of monomers that two surface loops in the region 203–221 were of different sizes and conformations in LDH and cMDH. Thus, although the LDH and MDH sequences have the same number of residues between 203 and 221, the loop conformations have markedly different consequences for subunit assembly. This result has not been apparent from simple sequence alignment alone.

Amino acid contacts across the *Q*, *P*, and *R* axes are given in Table II for the two crystallographic LDH tetramers and the model cMDH tetramer. Across an authentic subunit interface (*Q* axis) of the model structure, most contacts are in the 2–3.8-Å range and there are no forbidden contacts (<2 Å). As expected, there were many more contacts across the *Q* axis for the unregulated pig tetramer than for the regulated *B. stearothermophilus* tetramer. Again as expected, there were also many cross *R*-axis contacts in the pig enzyme which has an extended N-terminal arm which makes contact with *P*- and *R*-axis related subunits. Significantly, the modeled MDH tetramer had a large number (81) of forbidden contacts (<2 Å) across the *P* axis. These fell in four regions: region I, Gly178–Val186; region II, His202–Glu207; region III, Gly265–Phe269; and region IV, Lys300–Pro306. The most forbidden contacts occur between a loop in region II (Lys205B–Glu207, KNOBI) and region IV with less significant contacts between a loop in region III (Pro266B–Glu268, KNOBII) and region I (see Figure 2). Neither loop is present in either *B. stearothermophilus* or pig LDH. There are no conserved ion pairs in the *P*-axis interface with the exception of ionic bridges formed by the sulfate ions (in pig M_4) and the phosphate groups of FBP (in *B. stearothermophilus*) with residues Arg170 and His185A. These residues are both lysines in the equivalent region of cMDH and cannot interact in the same way with an anion bound at the *P* axis due to the differing length of the side chains (no anion is present at the *P* axis in the cMDH crystal structure). The analysis suggested a reason cMDH did not form a tetramer was the presence of bulky surface loops in regions II and III.

Template forced energy minimization showed no significant potential energy disadvantage in inserting the cMDH loops KNOBI and KNOBII (wild type with residues 264–269 being HGSPEGEI compared to wild-type HNENAI, an extra two residues) into bsLDH (results not shown). However, while the conformation of KNOBI was not much altered on energy minimization (rms change of unrestrained backbone atoms was 0.77 Å), that of KNOBII underwent a significant change (rms movement 2.87 Å).

The template forced loop conformations were modeled into the bsLDH crystal structure (see Materials and Methods) and subjected to energy minimization. The number of forbidden steric clashes (<2.0 Å) of KNOBI in the bsLDH model (23) was lower than in the model cMDH tetramer (53, see Table II). The number of forbidden contacts of KNOBII in bsLDH (10) was much lower than in the model cMDH tetramer (36) and four of these were resolvable by side-chain reorientation. Allowing the KNOBII loop to relax in the bsLDH crystal environment suggested it would not significantly inhibit tetramer formation.

The side chain of an inserted loop residue (Glu207) and that of His185A, one of the residues important for binding FBP (Wigley et al., 1992), moved to form an ion pair (Figure

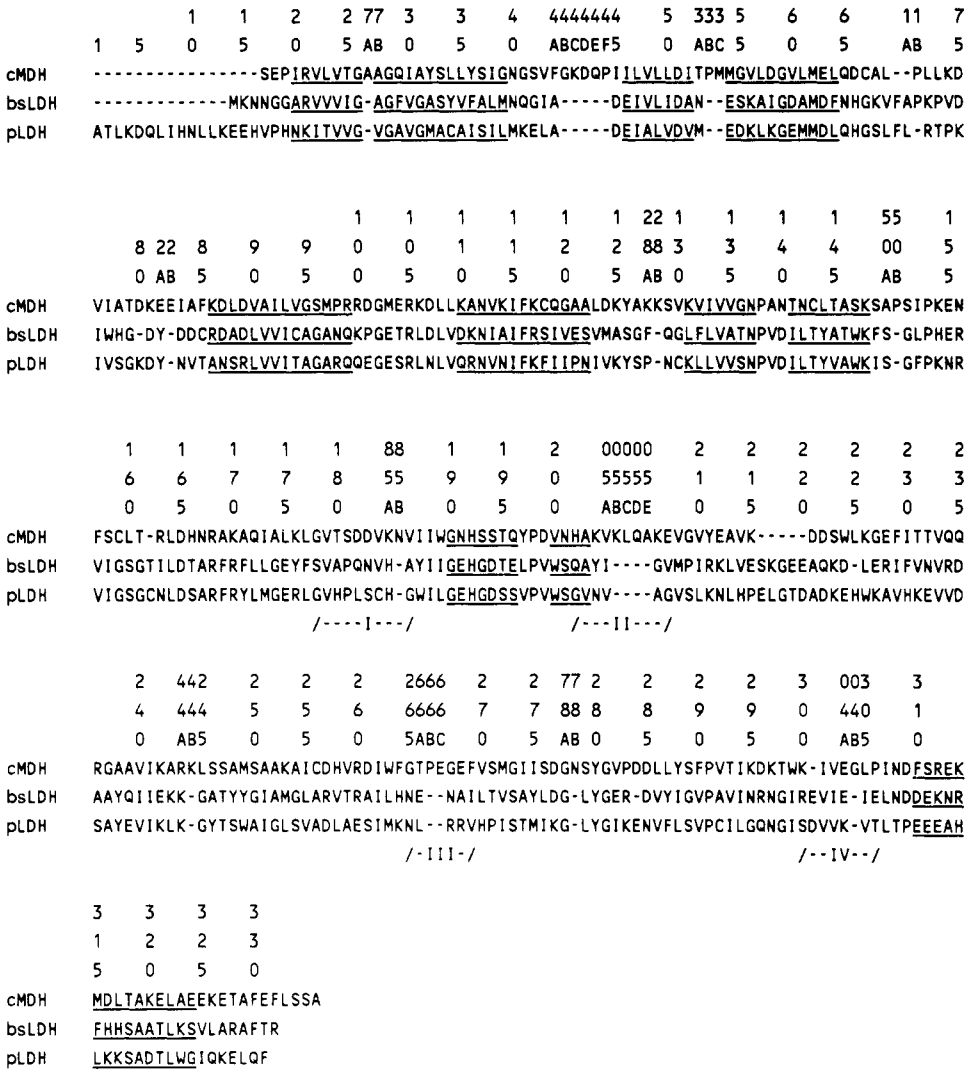

FIGURE 1: Alignment of the amino acid sequences of pig M_4 LDH, *B. stearothermophilus* LDH, and pig cMDH based upon superposing homologous regions of secondary structure (underlined). The alignment is numbered according to the pig LDH sequence. Regions I–IV form the *P*-axis contacts in the authentic pig LDH structure. The presence of a *P*-axis loop in MDH (gap in LDH at 266A–268) appears in most published alignments. However, secondary structure alignment reveals a new feature: although there are about the same number of residues between β-H (LDH 203) and α-1G (LDH 226), the best alignment is with a gap in LDH at 205B–205E (and a new, four-residue loop in MDH) and a gap in MDH at 216–220 (and correspondingly a loop in LDH). The underlined sequences were used to superpose the cMDH structure on the bsLDH and pLDH structures. cMDH is pig supernatant MDH. pLDH is pig M_4 LDH. bsLDH is *B. stearothermophilus* LDH.

3). This interaction would seriously hinder the binding of FBP to bsLDH containing KNOBI. The only other significant charge near the FBP binding site is Lys205B. In contrast to Glu207, this side chain points out of the FBP binding site, with the charged moiety completely solvent-exposed so its positive charge will not compensate for the deleterious effect of an ion-pair interaction between His185A and Glu207.

Enzymic Properties of the KNOBI Construct. Oligonucleotide mismatch mutagenesis was used to insert the new loop construction (Table I) into the wild-type *B. stearothermophilus* LDH structural gene using a technique which has been frequently used in this laboratory (Clarke et al., 1986b). The mutant protein (KNOBI) was purified to homogeneity in high yield using affinity chromatography. The affinity step depends on both the nucleotide and the substrate sites being functional. The success of the affinity step suggests, as planned, that this was so. This was confirmed when the steady state kinetics were measured (Table III). The k_{cat} and K_M values were very similar (without fructose 1,6-bisphosphate) to those of the wild type. This also suggests that altering the hydrophobic regions flanking the new loop to hydrophilic regions (to be stable when the *P*-axis face was exposed to water) was also successful. A similar conclusion could be drawn from the unchanged thermal stability of the construct.

The major difference in enzyme activity was seen in the presence of the allosteric activator fructose 1,6-bisphosphate. This ligand is the physiological activator of the *B. stearothermophilus* enzyme and functions by binding across the *P*-axis dimer between basic patches due to His185A and Arg170. The binding causes both tertiary and quaternary structure changes which activates metabolic flux through this enzyme due to the K_M for pyruvate being reduced from above the physiological concentration of substrate (4 mM) to well below it (50 μM; Clarke et al., 1986a). This effect in a slightly changed buffer system is seen again in Table III for the wild type. When the K_M for pyruvate tightens, the enzyme starts to show substrate inhibition with $K_{i(pyruvate)} \approx 20$ mM. KNOBI is, however, very different: it is significantly more active than the wild type, shows no measurable inhibition by pyruvate (a useful property for chemoenzymic transformations), and has the same high K_M as the unactivated enzymes. These effects were exactly those we should have predicted had the construction resulted in a stable dimer in which fructose 1,6-bisphosphate cannot bridge the *P* axis and stabilize a tetramer

Table II: Summary of the Amino Acid Contacts across the *P*, *Q*, and *R* Axes of Authentic and Modeled Dehydrogenases[a]

	no. of cross-axis contacts in the range				
	<1 Å	1–2 Å	2–3 Å	3–3.8 Å	total
bsLDH *Q*			4	33	37
bsLDH *P*			6	24	30
bsLDH *R*			2	11	13
pLDH *Q*			10	50	60
pLDH *P*			6	18	24
pLDH *R*			14	36	50
cMDH *Q*			13	41	54
cMDH *P*	21	60	49	84	214
cMDH *R*	9	19	20	42	90
cMDH					
region II	10	43	33	58	144
region III	14	22	22	23	81
model bsLDH					
KNOBI	8	15	32	22	77
KNOBII	4	6	12	17	39

[a] Summary of the amino acid contacts across the *P*, *Q*, and *R* axes of authentic *B. stearothermophilus* (bsLDH) and pig M_4 (pLDH) lactate dehydrogenase tetramers and the model pig cytosol malate dehydrogenase tetramer (cMDH) and lastly an analysis of contacts for regions II and III for cMDH and the corresponding KNOBI and KNOBII of the energy-minimized models (model bsLDH). Note: In the authentic tetramers there are no improper (<2 Å) collisions at the *P*- and *R*-intersubunit contacts, but there are many in the model *P*-axis tetramer of MDH.

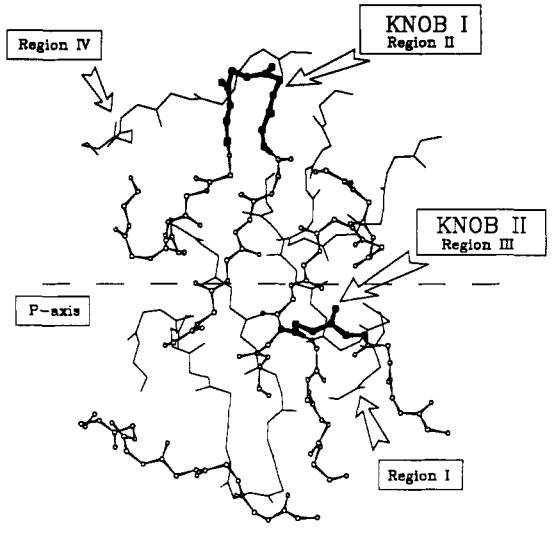

FIGURE 2: *P*-axis interface in the model cMDH tetramer. The contact region between two subunits, one from each MDH dimer, used to form a model cMDH tetramer is shown. One subunit is ball and stick, the other just sticks. The two loops, absent in LDH, are labeled KNOBI and KNOBII (thick lines). KNOBI collides with region IV (the loop between βM and αH). KNOBII collides with region I (the loop between α2F and βG). The *P* axis is shown projected onto the plane of the Figure.

(see Figure 3). More direct measures of subunit assembly were, however, needed to distinguish quaternary structure changes from changes in fructose 1,6-bisphosphate binding.

Estimation of Tetramer–Dimer Dissociation Constant from Time-Resolved Fluorescence Anisotropy. The time-resolved decay of the anisotropy of the fluorescence of the natural tryptophan fluorophores of *B. stearothermophilus* LDH has previously been used to reveal the presence of dimer and tetramer at low concentrations of *B. stearothermophilus* LDH (Clarke et al., 1985). The accuracy achievable with the large photon flux from a synchrotron radiation source makes the method ideal to measure protein assembly changes at low concentrations of protein especially when, as with LDH, there is a bright, long-lifetime (7 ns) tryptophan residue in the protein

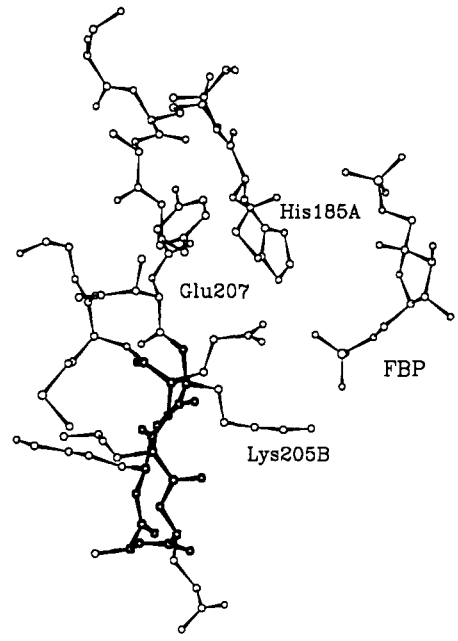

FIGURE 3: Putative FBP site in the KNOBI mutant of *B. stearothermophilus* LDH. The additional residues of KNOBI include both Lys205B and Glu207. The glutamate side chain forms an ion pair with His185A and would prevent binding of FBP. The lysine amine moiety is fully solvent-exposed and is not expected to influence FBP binding. The position of FBP shown is that found in the crystal structure of the wild-type enzyme (Wigley et al., 1992).

Table III: Steady-State Kinetic Constants of Wild-Type and KNOBI Mutant of LDH

	unactivated		+5 mM Fru-1,6-P_2				
enzyme	k_{cat} (s^{-1})	K_M (mM)	k_{cat} (s^{-1})	K_M (mM)	K_i (mM)	act.[a] (fold)	$t_{0.5}$ 90 °C (min)
KNOBI	268	5.2	262	4.9	>200	1.06	6
wild type	317	5.2	160	0.05	16	104	7

(Trp200). From the gel filtration results (see below) we expected the deconvoluted anisotropies to be due to two components. To estimate the limiting anisotropies of dimer and tetramer, the decay curves were first fitted to a single exponential decay with χ^2 values of 0.98–1.03. The rotational correlation times (ϕ_i) fell within a spread of 29–58 ns. The Stokes–Einstein function for a 23% hydrated protein, with partial specific volume 0.74 cm^3/g and viscosity 0.1194 P, predicts these limiting anistropies to be due to a spherical globule with molecular weight between 66 000 and 132 000 (Figure 4). The anisotropy decays were then reanalyzed for a two-exponential decay with the correlation times fixed at 29 and 58 ns to obtain the pre-exponential terms b_1 and b_2, respectively (Table IV). Since the fluorescence intensity of equal weights of the dimer and the tetramer differed by only about 15% (see below), the fraction of protein as dimer was set equal to $b_1/(b_1 + 0.5b_2)$ and that of tetramer as $b_2/2(b_1 + 0.5b_2)$. Three total protein concentrations, 1, 10, and 100 μM (33 000 subunits), were used both with and without 1 mM FBP in 20 mM BisTris–50 mM KCl buffer (pH 6) at 25 °C. The apparent equilibrium constant for the dimer to tetramer equilibrium was best estimated for those samples which contained appreciable fractions of both dimer and tetramer (Table IV).

At very low protein concentrations wild type type is an unstable dimer with a best estimate of $K_d = 20 \pm 5$ μM dimer. KNOBI, on the other hand, was a stable dimer with a best estimate of $K_d \geq 150 \pm 50$ μM dimer. In the presence of 1

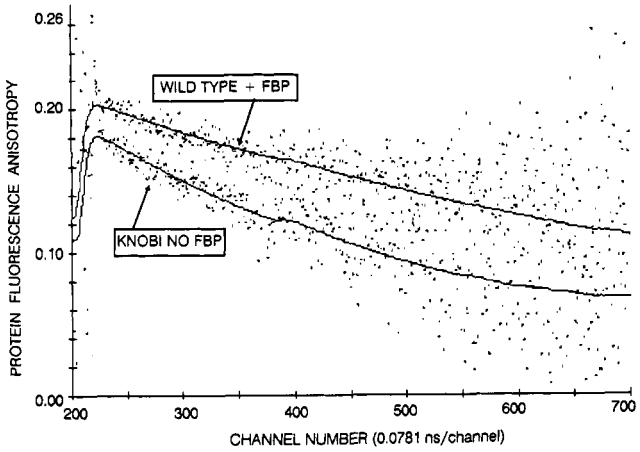

FIGURE 4: Comparison of the time-resolved decays of the protein fluorescence anisotropy of wild-type and KNOBI mutant of *B. stearothermophilus* LDH. Results were obtained as under Materials and Methods. Dots are experimental anisotropies. The lines are the deconvoluted fits with essentially 100% 58-ns correlation time (upper curve; 100 μM wild-type enzyme (subunits) with 1 mM FBP] and 29-ns correlation time (lower curve, 10 μM KNOBI mutant with no FBP). The synchrotron pulse width (200 ps) and photomultiplier response gave a fwhm of 400 ps.

Table IV: Analysis of the Time-Resolved Decay of Tryptophan Fluorescence Anisotropy (r) as a Mixture of 29- and 58-ns Components[a]

enzyme	b_1 29 ns	b_2 58 ns	χ^2	K (μM dimer)
10 μM WT	0.125	0.046	1.01	22.9
100 μM KNOBI	0.1269	0.067	1.056	150.0
1 μM WT + 1 mM FBP	0.0413	0.1481	1.123	0.10
100 μM KNOBI + 1 mM FBP	0.128	0.082	1.033	118.2

[a] Decays are represented as two exponentials $r_t = b_1e^{-t/29} + b_2e^{-t/58}$ (times in nanoseconds). The pre-exponential terms in the deconvoluted fit are b_1 and b_2. Protein concentrations are micromolar subunits. The calculated dissociation constant (K) for tetramer = 2 dimers is in units of micromolar dimer (M_r 66 000); results under other experimental conditions where there was not appreciable concentration of both dimer and tetramer were less accurate but consistent with the values shown.

mM fructose 1,6-bisphosphate wild type was stabilized as a tetramer with a best estimate of K_d = 90 ± 20 nM dimer (Table IV). Fructose 1,6-bisphosphate did not significantly reduce the K_d for KNOBI. The wild-type results agree with those of Clarke et al. (1986a). KNOBI had a much weakened *P*-axis contact and was insensitive to fructose 1,6-bisphosphate.

Estimation of Degree of Assembly from Gel Filtration. Gel filtration gave a direct demonstration that, as suggested by the steady-state enzyme results, wild type was a tetramer and KNOBI was a dimer (Figure 5). At 2.5 μM subunits the wild-type enzyme and KNOBI eluted from the gel filtration column at volumes corresponding to M_r 60 000 ± 5000 (i.e., mainly dimers). When 5 mM FBP was included in the eluting buffer, the elution volume decreased to correspond to M_r 100 000 ± 10 000 for wild type but was unaltered for KNOBI. At 80 μM without effector the elution volumes corresponded to M_r 100 000 (wild type) and 55 000 (KNOBI). At 120 μM without effector the elution volume for KNOBI corresponded to M_r 55 000. Although the method was not sufficiently precise to sensibly estimate a dimer–tetramer dissociation constant from the variation in average molecular weight with protein concentration, the conversion of wild-type dimer to tetramer and its separation from KNOBI dimer were easily demonstrated when the two samples at 2.5 μM were mixed and gel-filtered in the presence of 5 mM FBP (Figure 5).

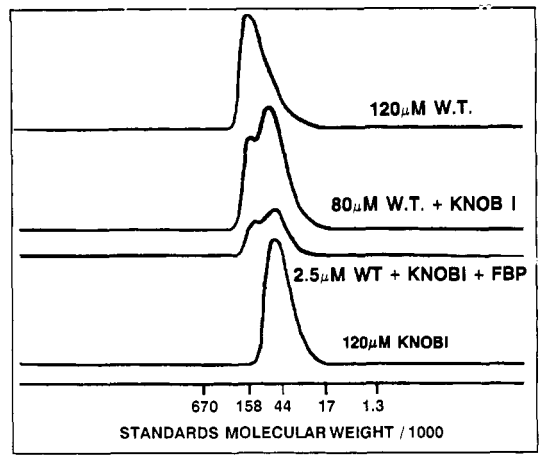

FIGURE 5: Gel filtration separation of the wild-type *B. stearothermophilus* LDH and KNOBI mutant. The apparent molecular weight of LDH was estimated using a Bio-Rad Bio-Sil TSK-250 HPLC gel filtration column. Initial protein concentrations (as monomers) are noted on the curves. The elution positions of Bio-Rad gel filtration molecular weight standards (151–1901), thyroglobulin, IgG, ovalbumin, myoglobulin, and cyanocobalamin are shown on the x axis.

Effects of FBP on Fluorescence at Equilibrium. At this point it was necessary to determine whether the insensitivity of KNOBI to fructose 1,6-bisphosphate was due to the inability to form a tight *P*-axis dimer or the loss of the fructose 1,6-bisphosphate site or both. The addition of FBP to *B. stearothermophilus* LDH causes a protein fluorescence enhancement. This enhancement was analyzed as being due to two effects: (a) tetramer formation altering protein fluorescence by shielding tryptophan residues [particularly Trp200 (Waldman et al., 1987), the main natural fluorophore] from the solvent as the subunit interface is formed; (b) FBP inducing a conformational change of each subunit which reduces the K_M of the active site for pyruvate. The environment of the tryptophan residues alters in this change.

If the magnitudes of these two changes can be distinguished, the effect of KNOBI mutation can be resolved into changes in assembly and changes in FBP binding. Distinction was possible for the wild type since at very high protein concentration the protein is all tetramer and the fluorescence change when FBP is added is the conformational contribution (about 4% increase). The increase induced by FBP at very low concentrations where the protein is mostly dimer is about 20%, and thus the first estimate of change due to tetramer formation is 20% – 4% = 16%.

Given these initial estimates of fluorescence coefficients, the effect of adding FBP at different protein concentrations (Figure 6) can be treated quantitatively

$$t = d + d \qquad K = d^2/t \qquad f = d/d_0$$

where K is the tetramer dissociation constant and d and t are the concentrations of dimer and tetramer, respectively, f is the mole fraction of protein as dimer, and d_0 is the total protein concentration expressed as dimer ($d_0 = d + 2t$). Mass conservation implies

$$f^2 2d_0 + fK - K = 0$$

which gives

$$f = (-K + (K^2 - 8d_0K)^{0.5})/4d_0 \qquad \text{(i)}$$

Using these estimates of fluorescence coefficients, the data in Figure 6 when fitted by a nonlinear regression to eq i using Grafit 2 (Leatherbarrow, 1991) yield a value of 11 μM for

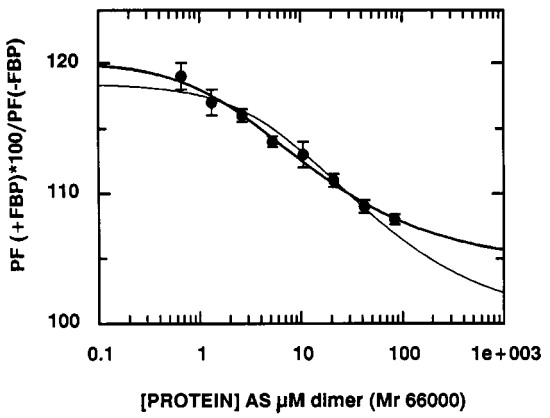

FIGURE 6: Protein concentration dependence of the FBP-induced protein fluorescence (PF) enhancement for wild-type LDH. FBP (5 mM) was added to a range of wild-type protein concentrations as shown. Percent increase in protein fluorescence (error bars are SD of the mean of four readings) was measured as described under Materials and Methods (●). The data were fitted as described under Results and Discussion. The bold curve is fitted to a tetramer dissociation constant of 11 μM in dimers. The limiting fluorescence changes are 104 and 120%. The fine curve is a fit with binding constant of 38 μM and the limiting fluorescence values of 118 and 100% (this was fixed). The fit curves are extended on a logarithmic abscissa and show the best fit with a high signal change to 104% is a better representation than one where there is no high protein signal change (100%).

the dissociation constant of tetramer. FBP-induced tetramerization causes a 20% increase in protein fluorescence. The FBP induced conformational change yields a 4% enhancement. The thin line in Figure 6 was a fit obtained with the high protein signal fixed at 100% (no change). The tetramerization signal and dissociation were allowed to vary (fit was 118% and 38 μM). This curve does not adequately fit the data and shows that FBP when it binds to the tetramer does give a small fluorescence enhancement. The K_d value of 11 μM may be compared to a value of 33 μM determined previously in a slightly different buffer system (Clarke et al., 1986a).

Adding 1 mM FBP to 50 μM KNOBI mutant showed no (±1%) change in fluorescence. Increasing FBP to 10 mM had little effect. These results show that FBP can neither induce KNOBI to form tetramer (in accordance with the time-resolved anisotropy and gel filtration results) nor bind to it in a way which gives the 4% fluorescence increase seen in wild-type enzyme. This confirms the steady-state kinetics, where no FBP induced reduction of K_m for pyruvate is observed in KNOBI. The simplest explanation for these data is that the FBP site in KNOBI is not occupied. Since the affinity for FBP appears to be even lower for KNOBI than for the *B. stearothermophilus* LDH dimer (3 mM; Clarke et al., 1986a), it must be assumed that the presence of the inserted loop and in particular the presence of Glu207 (identified in the modeling study) abolish FBP binding to the dimeric state.

At this point we should recall the analysis made of some factors which result in cMDHs being dimers and LDHs being tetramers. Two surface loops were identified on MDH (KNOBI and KNOBII), one of which, when modeled by molecular graphics, was stable enough to prevent the two MDH dimers from coming together to form a stable tetramer like LDH. When this loop was added to LDH, we observed that KNOBI prevented tetramer formation, as expected from the analysis. After this work was completed, we noted other observations which suggest the KNOBII region may not be significant for inhibiting tetramer formation. There are now gene-derived amino acid sequences for three plant MDHs (Scheibe et al., 1991; Metzler et al., 1989; Cretin et al., 1990). All have the sequence insert KNOBII, and maize, pea, and spinach $NADP^+$-MDH have been described as tetramers under gel filtration conditions.

The conclusion to this study is that LDHs are tetramers and cMDHs are dimers in part because of the absence of the interdimer *R*-axis arm in MDHs and in part because the colliding residues at the *P* axis of MDH inhibit the formation of a LDH-like tetramer. One extra *P*-axis sequence region forms a stable loop which collides with the next dimer and prevents the close approach required for a *P*-axis tetramer in LDH. This loop (203–207) also prevents the formation of a tetramer-stabilizing bridge across the *P* axis by the bidentate anion fructose 1,6-bisphosphate. The absence of a cDNA expression and mutagenesis system for cMDH means it is not presently possible to experimentally test whether there are other factors, such as the different hydrophobicity of the subunit interfaces, which determine the dimeric nature of cMDH.

REFERENCES

Banaszak, L. J., & Bradshaw, R. A. (1975) *Enzymes (3rd Ed.) 11A*, 369–396.

Barstow, D., Clarke, A. R., Chia, W. N., Wigley, D., Sharman, A. F., Atkinson, T., Minton, N. P., & Holbrook, J. J. (1986) *Gene 46*, 47–55.

Bernstein, F. C., Koetzle, T. F., Williams, G. J. B., Meyer, E. F., Brice, M. D., Rodgers, J. R., Kennard, O., Shimanouchi, T., & Tasumi, M. (1977) *J. Mol. Biol. 112*, 535–542.

Birktoft, J. J., Rhodes, G., & Banaszak, L. J. (1989) *Biochemistry 28*, 6065–6081.

Brosius, J., & Holy, A. (1984) *Proc. Natl. Acad. Sci. U.S.A. 81*, 6929–6933.

Carter, P., Bedouelle, H., & Winter, G. (1985) *Nucleic Acids Res. 13*, 4431–4443.

Clarke, A. R., Waldman, A. D. B., Munro, I., & Holbrook, J. J. (1985) *Biochim. Biophys. Acta 828*, 375–379.

Clarke, A. R., Evington, J. R. N., Dunn, C. R., Atkinson, T., & Holbrook, J. J. (1986a) *Biochim. Biophys. Acta 870*, 112–126.

Clarke, A. R., Wigley, D. B., Chia, W. N., Barstow, D., Atkinson, T., & Holbrook, J. J. (1986b) *Nature 324*, 699–702.

Clarke, A. R., Atkinson, T., & Holbrook, J. J. (1989) *Trends Biochem. Sci. 14*, 145–148.

Cretin, C., Luchetta, P., Joly, C., Decottignies, P., Lepiniec, L., Gadal, P., Sallantin, M., Huet, J-C., & Perrnollet, J-C. (1990) *Eur. J. Biochem. 192*, 299–303.

Dauber-Osguthorpe, P., Roberts, V. A., Osguthorpe, D. J., Wolff, J., Genest, M. G., & Hagler, A. T. (1988) *Protein Struct., Funct. Genet. 4*, 37–47.

Dunn, C. R., Wilks, H. M., Halsall, D. J., Atkinson, T., Clarke, A. R., Muirhead, H., & Holbrook, J. J. (1991) *Philos. Trans. R. Soc. (London) B 332*, 177–185.

Holbrook, J. J., Liljas, A., Steindel, S. J., & Rossmann, M. G. (1975) *Enzymes (3rd Ed.) 11A*, 191–292.

Jeckel, D., Anders, R., & Pfleiderer, G. (1973) *Hoppe Seyler's Z. Physiol. Chem. 354*, 737–782.

Leatherbarrow, R. J. (1990) Grafit v. 2.0, Erithracus Software Ltd., Staines, U.K.

Marquart, D. W. (1963) *J. Soc. Ind. Appl. Math. 11*, 431–441.

Metzler, M. C., Beverley, A., Rothermel, A., & Nelson, T. (1989) *Plant Mol. Biol. 12*, 713–722.

Messing, J., & Vieira, J. (1982) *Gene 19*, 269–276.

Opitz, U., Rudolf, R., Jaenicke, R., Ericson, L., & Neurath, H. (1981) *Biochemistry 26*, 1399–1406.

Pfleiderer, G., Nagel, G., & Buehler, H. (1991) *Experientia 47*, 470–475.

Rossmann, M. G., Liljas, A., Brandén, C.-I., & Banaszak, L. J. (1975) *Enzymes (3rd Ed.) 11A*, 61–102.

Sambrook, J., Fritsch, E. F., & Maniatis, T. (1989) *Molecular Cloning—a laboratory manual*, 2nd ed., Cold Spring Harbor Laboratory Press, Cold Spring Harbor, NY.

Sanger, F., Coulson, A. R., Barrell, B. G., Smith, A. J. H., & Roe, B. A. (1980) *J. Mol. Biol. 143*, 161–178.

Scheibe, R., Kampfenkel, K., Wessels, R., & Tripier, D. (1991) *Biochim. Biophys. Acta 1076*, 1–8.

Steffan, J. S., & McAlister-Henn, L. (1991) *Arch. Biochem. Biophys. 287*, 276–282.

Struthers, R. S., Rivier, J., & Hagler, A. T. (1984) in *Conformationally directed drug design: Peptides and Nucleic Acids as Templates or Targets* (Vida, J. A., & Gordon, M., Eds.) pp 239–261, American Chemical Society, Washington, DC.

Waldman, A. D. B., Clarke, A. R., Wigley, D. B., Hart, K. W., Chia, W. N., Barstow, D. A., Atkinson, T., Munro, I., & Holbrook, J. J. (1987) *Biochim. Biophys. Acta 913*, 66–71.

Wigley, D. B., Gamblin, S. J., Turkenburg, J. P., Dodson, E. J., Piontek, K., Muirhead, H., & Holbrook, J. J. (1992) *J. Mol. Biol. 223*, 317–335.

Registry No. MDH, 9001-64-3; LDH, 9001-60-9; FBP, 488-69-7; pyruvic acid, 127-17-3.